Document Delivery - Monash University Library

PAC-10086996

VMOU

SUBITO

GREG SHEARD
CLAYTON CAMPUS
MONASH UNIVERSITY LIBRARY
ARIEL.LIB.MONASH.EDU.AU; DOCUMENT.DELIVERY@MONASH.EDU
MECHANICAL AND AEROSPACE ENGINEERING
FACULTY OF ENGINEERING

ATTN:
PHONE: +61399051182
FAX:
E-MAIL:

SUBMITTED: 2011-04-30 13:07:34
PRINTED: 2011-05-04 14:21:23
REQUEST NO.: PAC-10086996
SENT VIA: World Wide Web
PATRON TYPE: Staff

PAC Core Copy Journal

TITLE:	AERONAUTICAL JOURNAL
VOLUME/ISSUE/PAGES:	114 (1158) 485-492
DATE:	2010
AUTHOR OF ARTICLE:	Watkins, S., Thompson, M., Shortis, M., Segal, R., Abdulrahim, M. & Sheridan, J.
TITLE OF ARTICLE:	AN OVERVIEW OF EXPERIMENTS ON THE DYNAMIC SENSITIVITY OF MAVS TO TURBULENCE
ISSN:	0001-9240
DELIVERY:	E-mail Post to Web: greg.sheard@monash.edu
REPLY:	E-mail: greg.sheard@monash.edu

If you have further queries regarding this request please contact

Document Delivery - Monash University Library

PAC-10086996

Document delivery at Document.Delivery@monash.edu or phone + 61 3 9905 2679, quoting your request number.

Materials provided with this request have been copied pursuant to Section 49 or 50 of the Copyright Act as amended, on behalf of Monash University LibaBldg 4, Wellington Rd, Monash University, Clayton, VIC 3800

An overview of experiments on the dynamic sensitivity of MAVs to turbulence

S. Watkins
simon@rmit.edu.au
M. Thompson, M. Shortis and R. Segal
RMIT University, Australia

M. Abdulrahim
University of Florida
Florida, USA

J. Sheridan
Monash University
Australia

ABSTRACT

Aspects of the turbulent wind environment Micro Air Vehicles (MAVs) experience when flying outdoors were replicated in a large wind tunnel. An overview of the facility, instrumentation and initial flight tests is given. Piloting inputs and aircraft accelerations were recorded on fixed and rotary wing MAVs and for some tests, measurements of the approach flow (*u,v,w* sampled at 1,250Hz at four laterally disposed upstream locations) were made. The piloting aim was to hold straight and level flight in the 12m wide × 4m high × ~50m long test section, while flying in a range of turbulent conditions. The Cooper-Harper rating system showed that a rotary craft was less sensitive to the effects of turbulence compared to the fixed wing craft and that while the fixed wing aircraft was relatively easy to fly in smooth air, it became extremely difficult to fly under high turbulence conditions. The rotary craft, while more difficult to fly per. se., did not become significantly harder to fly in relatively high turbulence levels. However the rotary craft had a higher mass and MOI than the fixed wing craft and further work is planned to understand the effects of these differences.

1.0 INTRODUCTION AND AIMS

Whilst the miniaturization of the propulsion and control technology has enabled more sophisticated systems to be developed for MAVs, a significant challenge is now posed by the flight environment; particularly as the scale of the craft reduces. Like their natural counterparts, MAVs are of light weight and have low moments of inertia, which, when coupled with their small size, makes them very prone to disturbances from turbulence. Unlike their natural counterparts they generally cannot rapidly respond and correct for the dynamic inputs arising from their turbulent flight environment. Much of the current work on MAVs utilise human pilots where it is well known that the maximum frequency of human control response time is far lower than that encountered in small birds and insects. Thus new challenges in aircraft and control system design arise which need to be addressed if MAVs are to attain the level of utility of the larger unmanned craft. A framework to provide information enabling better utility of MAVs is given in Fig. 1.

MAV operations are of short duration, at low speed and are close to the ground. For their entire flight duration MAVs are thus immersed in the lower part of the Atmospheric Boundary Layer (ABL) and for an appreciable part of the flight duration are operating in what wind engineers term the roughness zone, where the wakes of the local surface obstructions are significant. One of the key advantages of a MAV is to offer additional information other than that afforded by direct line of sight, i.e. flown over hillsides, around street corners or up to a window for reconnaissance and surveillance, Burger [1]. Thus the operating environment is one which can involve flights over, around or through natural and man made objects. The wind environment of cities is known to be complex and the wakes of ground-based objects increase the turbulent energy levels in the ABL. When the atmospheric wind is present, the operational flow environments of MAVs are turbulent; far more so than for larger aircraft that cruise well above the ABL.

Paper No. 3522. Manuscript received 7 January 2010, accepted 25 March 2010.

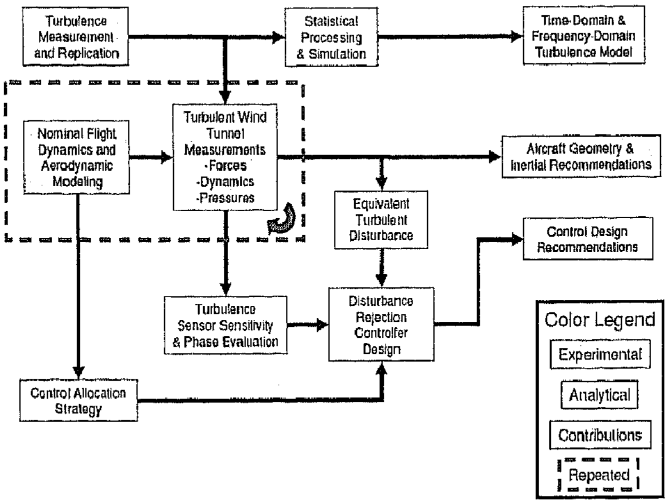

Figure 1. Framework of enabling technology for enhanced MAVs.

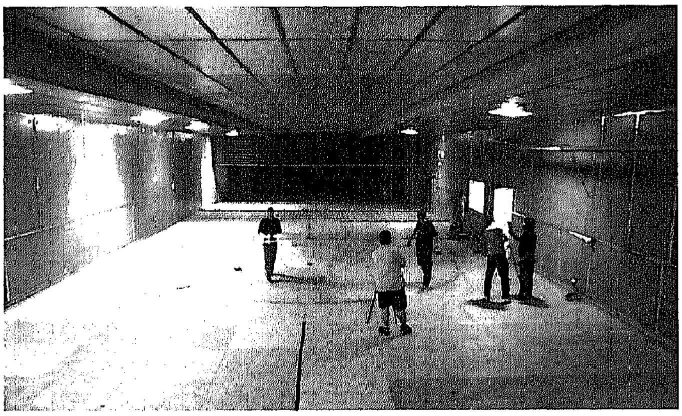

Figure 2. The wind engineering test section, looking upstream towards the turntable.

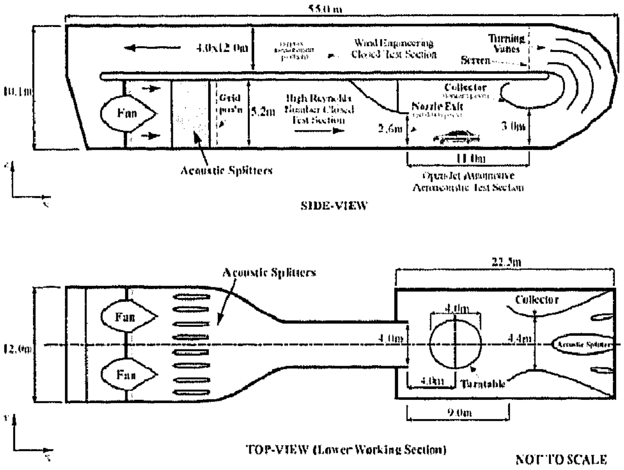

Figure 3. Flight test facility: overview.

Experience from piloting MAVs has shown that one of the largest challenges to outdoor MAV flight is overcoming the effects of turbulence, particularly small vortices and eddies that are inherent in atmospheric turbulence and that produce seemingly random roll and pitch inputs. This is due to the relative size of eddy structures in atmospheric turbulence with respect to MAVs. The resultant roll and pitch instabilities hinder operability in critical situations and thus would curtail the number of possible days per year that they could be used for outdoor activities.

The atmospheric wind environment has been studied in detail over much of the past century by wind engineers and meteorologists (e.g. Refs 2-5) although generally at much longer or larger scales, (temporal and spatial) than is desirable or required for MAVs. Data were obtained via large-scale, fixed (with respect to the Earth) anemometers and the frame of reference is the wind axis. For vehicles moving through the ABL, the interest is in the frame of reference with respect to the moving vehicle. Our recent work has focused on building an understanding of the turbulent flight environment within the ABL with respect to the moving aircraft. Since the scales relevant to small flying aircraft, birds and insects are small, our focus has been on measuring and understanding the finer scale turbulent structures found in the lower region of the ABL, see Watkins *et al*[6]. This study is described in previous work, Milbank *et al*[7] where the authors gathered data by mounting a bank of multi-hole pressure probes onto a mast above a car, 4m above the road, and 'flying' them through the atmosphere under a range of different wind speeds, conditions and through different terrains.

It is evident that in order to design an MAV (including associated control systems) capable of successful outdoor flight in windy conditions, a development environment that can simulate or replicate aspects of conditions found in the lower parts of the ABL is desirable. While it is considered that simulation in the computational domain (CFD) would provide a useful development environment for this task, the computation necessary to accurately replicate such complex flow fields is not yet available. This leaves experimental methods as the only practical solution, at least for the next few years. By adapting a wind tunnel facility to replicate aspects of turbulence found over a range of terrains and wind conditions, a more detailed analysis of a MAVs ability to achieve its mission objectives can be made. Note that such replication techniques have been commonplace for the study of flows around and loads on buildings for several decades.

We have created a repeatable, controllable turbulent environment for the study of man-made MAVs and perhaps birds and the larger flying insects, initially described in Watkins *et al*[9]. By reconfiguring a large industrial wind tunnel, and using a selection of grids and screens, we produced a range of turbulence intensities and integral length scales and considered that these conditions cover the majority of turbulent flow conditions relevant to MAVs flying in a typical range of wind speeds in complex terrain. Our studies are restricted to well mixed turbulent flow, rather than investigating discreet gusts and local effects (such as might be found in extremely close proximity to buildings etc.). The work described here forms part of a larger program which is focused on determining the influence of MAV type (fixed wing, rotary and flapping) on ability to fly in relatively turbulent flow conditions. Manned craft have received much attention with respect to the effects of atmospheric turbulence but generally this is clear-air turbulence at high altitude.

It is interesting to note that in a 1981 Wright Brothers Memorial Lecture, Etkin[8] foresaw the requirement to make measurements from laterally separated probes, in order to study the effects on manned aircraft taking off and landing in windy conditions. This was well before the advent of MAVs. He suggested a series of measurements at the maximum frequencies of interest, made at points representing the path of the aircraft through a variety of atmospheric conditions to enable a further understanding of the disturbances. Etkin noted that the turbulence present in the atmosphere is composed of two components; discrete gust inputs and random continuous turbulence. The former are local events with obvious causes, such as traversing the near wake of a large building. The latter can be described as a chaotic motion of the air that needs to be described via its statistical properties.

In this paper we describe the systems and techniques involved with the experimental replication of the turbulent flight environments and the instrumented MAVs. We only give preliminary results of our flight trials flying fixed and rotary wing MAVs in the facility, since the dynamic sensitivity studies are published separately.

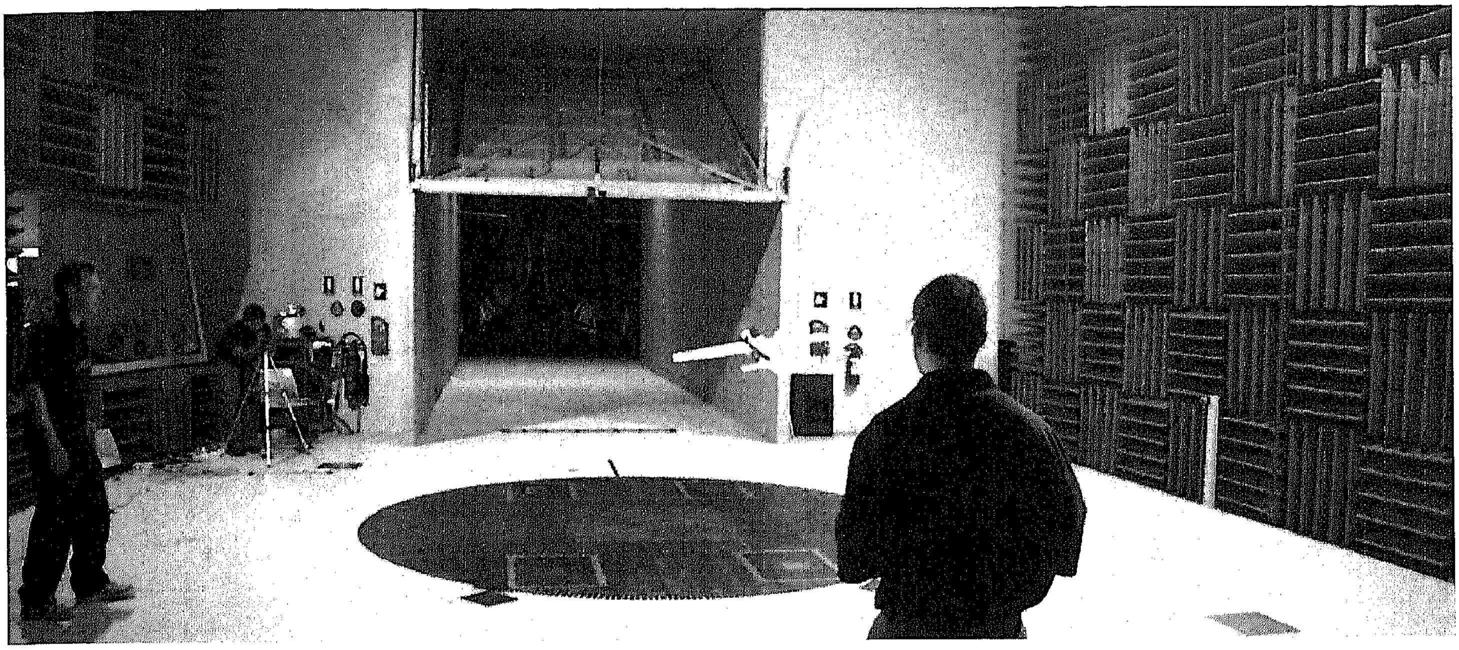

Figure 4. Flying in the automotive test section looking towards the nozzle exit.

2.0 THE FLIGHT TEST FACILITY

The facility used was a large industrial wind tunnel located at Monash University in Melbourne. This is the largest wind tunnel in the Southern Hemisphere, and is sufficiently large to permit flight of MAVs of up to about 1m span. The tunnel is driven by two 5m diameter, fixed pitch, variable speed, axial fans situated at the start of the lower circuit. The upper test section can be seen in Fig. 2.

A schematic of the wind tunnel is shown in Fig. 3. The wind tunnel is of the closed circuit type, and was designed as a multiple use facility with three working sections: (*i*) an open-jet automotive aeroacoustic test section on the lower level; (*ii*) a general purpose high Reynolds number closed test section, also on the lower level and (*iii*) a wind engineering, closed test section on the upper level.

The automotive test section provides a low turbulence level area for flying in relatively smooth air (longitudinal turbulence intensity ~1·5%). It also offers the opportunity for craft to fly from the relatively stationary air (in the plenum chamber) into the jet, thus permitting a step change in flight speed – from either side of the jet, or from above. An aircraft can be seen flying in the open jet of the automotive test section in Fig. 4 and the surrounding plenum chamber can be seen bordered by anechoic wedges.

As the focus of our work is to understand the effects of turbulence the majority of tests were carried out in the wind engineering section on the upper level of the tunnel. This has a 4m high by 12m wide by approximately 50m long test section and an 8m diameter turntable. It is commonly used for simulations of the ABL in wind engineering studies, see Fig. 2

The wind engineering test section can be configured to give a wide range of turbulence characteristics by changing the screens at the entrance of the section, combined with changes to the lower part of the tunnel. As well as the conventional method of utilising grids, other changes include varying the nozzle exit elevation and the collector position, see Fig. 1. These changes permit the generation of turbulence intensities up to 25% in the wind engineering tests section, with longitudinal integral length scales of up to 1·7m.

For this work two tunnel configurations were used; Configuration A, which gave a longitudinal turbulence intensity of 6·6%, with an integral length scale of 0·87m; and Configuration B which gave a longitudinal turbulence intensity of 14·0% and an integral length scale of 1·69m. It should be noted that a very wide range of relative turbulence characteristics can be experienced by flight under a range of aircraft and atmos-

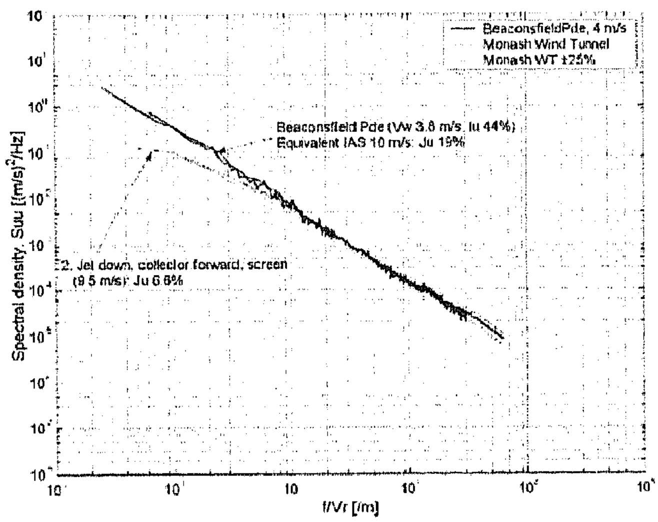

Figure 5. Spectral density *vs* wave number for tunnel compared with outdoor measurements In A 3·8m/s^{-1} atmospheric wind, built-up urban area, 2-3 Storey Buildings, From Watkins *et al*[9].

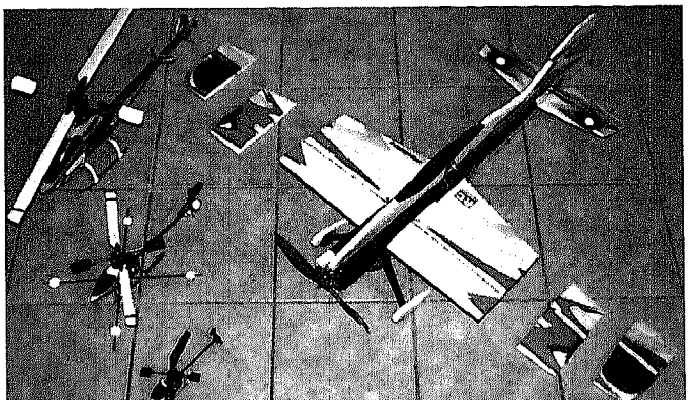

Figure 6. The flash fixed wing craft showing span modifications and three rotary craft.

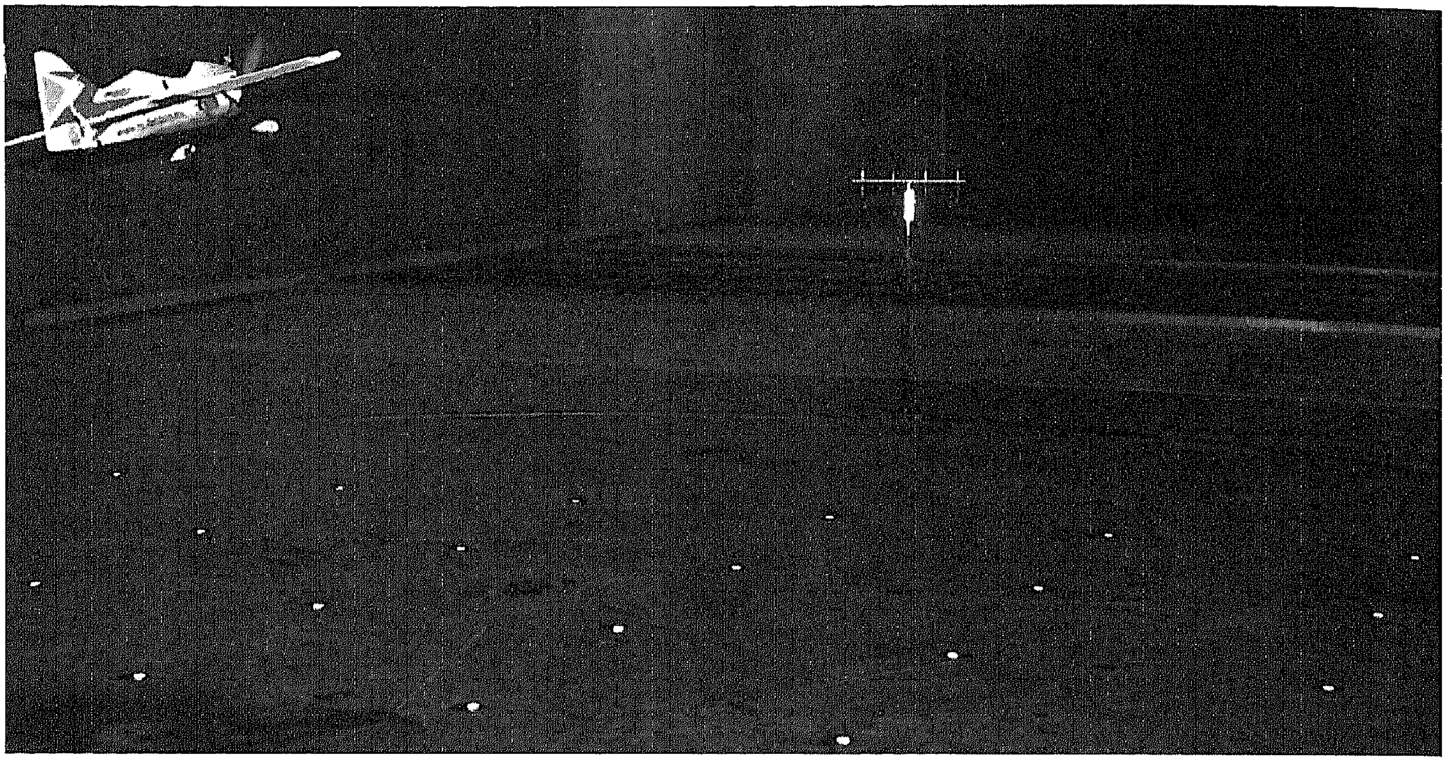

Figure 7. Fixed wing craft approaching the centre turntable position, note cobra probe bank upstream and reflective ground markers for video tracking.

pheric wind speeds – this has been detailed in our prior work, Watkins[6]. Figure 5 depicts the spectrum of turbulence for Configuration B and also a comparison with that experienced by flight of $10ms^{-1}$ IAS through a built up urban area when flying into a $3{\cdot}8ms^{-1}$ atmospheric wind. This wind speed is thought to be close to an average mean value for an elevation of about 4m for non-cyclonic areas, Watkins[10]. It can be seen that the turbulence follows the well known 5/3rds Kolmogorov spectral decay. Further details of the various tunnel configurations, associated turbulence characteristics and comparison with outdoor measurements can be found in Milbank *et al*[7].

3.0 TEST AIRCRAFT AND PROCEDURES

In initial tests we examined the influence of fixed vs rotary craft on the piloting workload while attempting to hold straight and level (SL) flight over the turntable centre of the wind engineering section, Watkins *et al* [11]. In our current research program we have conducted a more exhaustive series of tests, these include investigating;

- controllability of a fixed wing MAV *vs* a rotary wing (initial findings reported in this paper);
- the influence of MAV scale (rotary and fixed wing) to turbulence scale;
- the link between the upstream velocity fluctuation and the MAV response, and;
- the effect of mass and MOI changes on response and controllability.

The fixed wing craft was a 'Flash' which is a commercially available model, modified via changes to the span, mass and MOI about the roll axis. Three different scales of helicopter were used; the helicopter used for the results reported here was the largest of the three; a commercially available 'Blade 400'. This helicopter is of standard configuration, with twin-blade single main rotor, a tail rotor, and Bell-Hiller system on the main rotor. All aircraft were radio-controlled using commercially available components and for the tests reported here there were no inputs to the flight control systems other than the visually based piloting commands. Models can be seen in Fig. 6.

4.0 DATA ACQUISITION – FLOW MEASUREMENT

The same system used in the prior outdoor testing was utilised, for details see Milbank *et al*[7]. This configuration consisted of four Cobra Probes mounted on an aerodynamically faired bracket, equally spaced in the lateral direction with a separation of 150mm, thus giving a total span of 450mm. The bracket with probes was mounted on the centerline of the wind engineering test section in order to check the statistical properties of the flow and, for some flight experiments, measure the instantaneous turbulent flow field upstream of the flying position, see Fig. 7.

Measurement samples were typically several minutes in length and data were acquired at 5kHz and then filtered and down sampled to 1·25kHz to avoid aliasing effects. Processing consisted of calculating the relevant statistics (mean values, standard deviations and turbulence intensity), followed by the power spectral density versus normalised frequency (in this case wave number, $k = f/Vr$).

For some tests, data from the four upstream probes were concurrently obtained with the flight data from the aircraft inertial system and pilot control inputs, as well as the video tracking system (see later). These will be analysed to understand the relationship between the turbulent flow inputs and the aircraft dynamics and control.

5.0 DATA ACQUISITION – AIRCRAFT INERTIAL SYSTEM AND PILOT CONTROL INPUTS

A modular approach was taken in the design of the instrumentation system. A sensor unit comprised of three orthogonal linear accelerometers and three orthogonal angular rate sensors interfaced to a miniature data acquisition unit. Analog voltages generated by the sensors were filtered and sampled by a 12-bit analog-to-digital converter on the data acquisition board. The converter was multiplexed to allow measurement of 16 single-ended input channels. Conversion results were processed by a microcontroller and recorded to an on-board flash memory module.

A sampling rate of 100Hz was chosen which was thought to be sufficiently high relative to the expected frequency content of interest. Analog filtering used for each channel was with a simple single-pole RC filter whose corner frequency varies from 5Hz on low-frequency versions of the data acquisition board, to 25Hz for high-frequency versions. While each sensor measurement contained 12-bits of useful information, the data were sent as a 2-byte sequence to simplify handling. Two bytes from each of 16 input channels plus chip temperature measurement and a 3-byte data frame marker resulted in 37 bytes at 100Hz, which yielded a data rate of 3,700 bytes per second. At this rate, the memory capacity was sufficient for 19 minutes of sampling, which exceeded the flight duration of most of the tested aircraft.

The weight and footprint of the data acquisition board were driven largely by the choice of interface connectors, which themselves were based on convenience and usability. The board versions used in the flight trials use standard 0·1" pin-spacing connectors, which occupy a large portion of the board area due to the large number of input channels. The data acquisition board weighed 17 grams and interfaces to the connectors commonly used for UAVs. An alternate version of the board uses connectors with 0·05" pin-spacing connectors and weighs 6 grams. This board is intended for future trials with smaller MAVs.

6.0 DATA ACQUISITION – VIDEO TRACKING

The use of multiple video cameras to track the location and attitude of aerospace models in wind tunnels is a well established technique Shortis and Snow[12]. In this instance video tracking was also utilised; this allowed the derived lateral and rotational movements of the aircraft to be doc umented and compared with the data from the onboard Data Acquisition (DAQ) modules. This is planned for future research on the smaller craft that would not support the weight of the smallest DAQ.

Six video camcorders were rigidly mounted to the ceiling of the tunnel to provide a reasonable coverage of the flight volume while still giving a resolution of 3-5mm for lateral movements and 0·5 degrees for rotations. Retro-reflective targets were placed in a grid pattern on the floor of the tunnel to provide highly visible points to determine the relative locations and orientations of the six cameras. Retro-reflective targets were placed on the flight surfaces of the fixed wing craft and on the undercarriage of the helicopters to enable tracking of the position and attitude of the vehicles relative to the base plane of the wind tunnel, see Fig. 7.

Synchronisation was achieved using a flashing LED placed in view of all cameras and with the use of an external flash gun at random times throughout each test. Selected image sequences from the six camcorders were then analysed using the VMS software package from Geometric Software (see http://www.geomsoft.com).

7.0 FLIGHT TESTING PROCEDURE

The tunnel was set to the average flying speed of the aircraft and they took off from a location approximately 2/3rds down the test section working length. They were then flown at slightly above tunnel speed until they were located at a reference position over the turntable location at mid test section height and width, approximately 4m downstream of the Cobra Probes. Here the pilot attempted steady straight and level flight directly downstream of the Cobra Probes and within the viewing location of the six overhead video cameras. The aircraft were held within ±1m from the reference position in the longitudinal and vertical directions, whereas lateral deviations were ±2m. Depending upon the aircraft type and configuration and tunnel turbulence level, differing amounts of control inputs were required to keep the aircraft as level as possible and visually aligned behind the probes. Interaction between pilot and tunnel speed was required in the initial flights, since the flying speed of the aircraft was not known exactly.

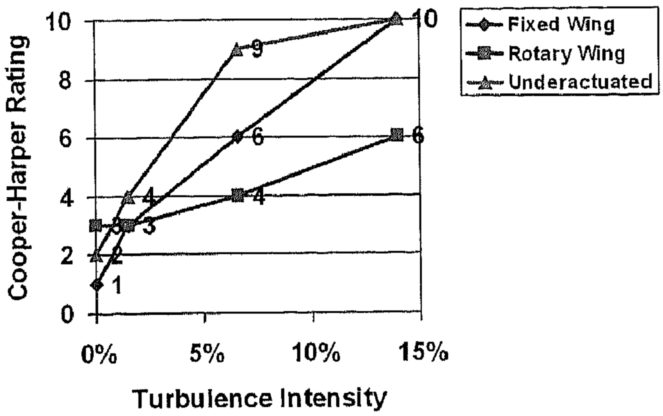

Figure 8. Cooper-Harper rating as a function of turbulence intensity.

As well as comparing subjectively and objectively the control inputs and responses of the unmodified fixed and rotary aircraft, several parameters were varied on the fixed wing craft. These were mass, MOI about the roll axis, wing loading and span. The results of this parametric variation will be given in future papers.

8.0 RESULTS AND DISCUSSION

A large data set was obtained from the tests and is currently being analysed using standard control theory and spectral analysis, see Abdulrahim *et al*[13]. Here we give an assessment of the handling qualities described via the Cooper-Harper rating scale (C-H). A highly skilled pilot with extensive manned and radio-control experience flew all flights and gave a rating shortly after each flight. A C-H rating of 1 corresponds to excellent and highly desirable handling qualities; whereas a rating of ten corresponds to major deficiencies where control will be lost (C-H rating is commonly used for manned aircraft; for details see http://history.nasa.gov/SP-3300/fig66.htm).

In smooth flow (~1·5% turbulence intensity in the Automotive Test Section and outdoor flying in calm conditions) the pilot judged the fixed and rotary wing craft at a C-H rating of 1-3 with minimal to moderate pilot compensation required. When the turbulence level was 6·6% (in the Wind Engineering Section) the ratings were 5-6 for the fixed wing ("adequate performance, requires considerable to extensive pilot effort") and 4 for the rotary wing ("moderate pilot compensation required for desired performance"). When the turbulence level was raised further to 14% the rating was 10 for the fixed wing ("considerable to intense pilot compensation required, control was always lost at some point") and 5-6 for the rotary wing ("adequate performance, requires considerable to extensive pilot effort").

The difficulty associated with piloting fixed-wing MAVs in turbulence can be inferred from the flight data shown in Fig. 9. Standard inertial response measurements are shown along with piloted stick inputs for the fixed wing craft with standard weight and CG location. The task was simply to maintain straight and level flight downstream of the Cobra probe bank. Pilot commands were made to reject the attitude disturbances due to turbulence and return the aircraft to the desired position in the tunnel. Note that for some data sets there are two traces (e.g. Aileron and Aileron 2 in Fig. 8); this is due to redundancy in data acquisition and the two traces are closely similar.

The upper linear acceleration plot shows the aircraft sustaining large vertical acceleration motion and smaller perturbations along the longitudinal and lateral axes. Some of the motion appears

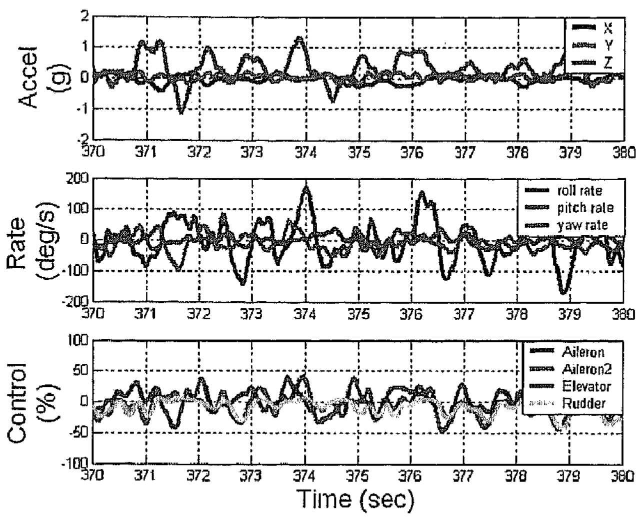

Figure 9. A 10-second time history of flight data from the fixed wing aircraft flown in a turbulence intensity 6·6% for an IAS of 7·5m/s^{-1}.

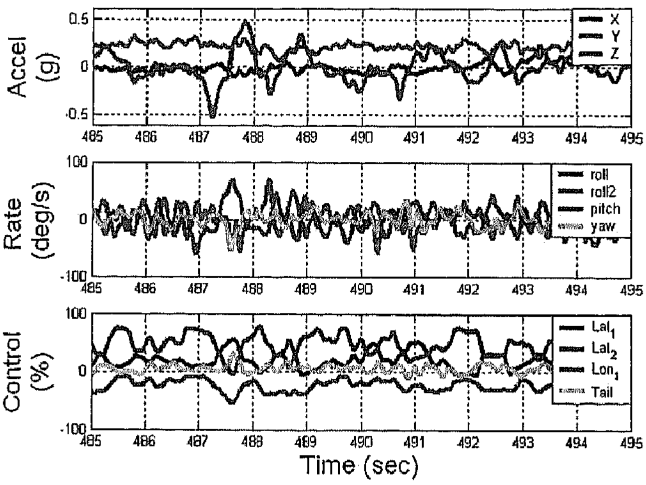

Figure 10. A 10-second time history of flight data from the helicopter flown in a turbulence intensity 6·6% For an IAS of 7·5m/s^{-1}.

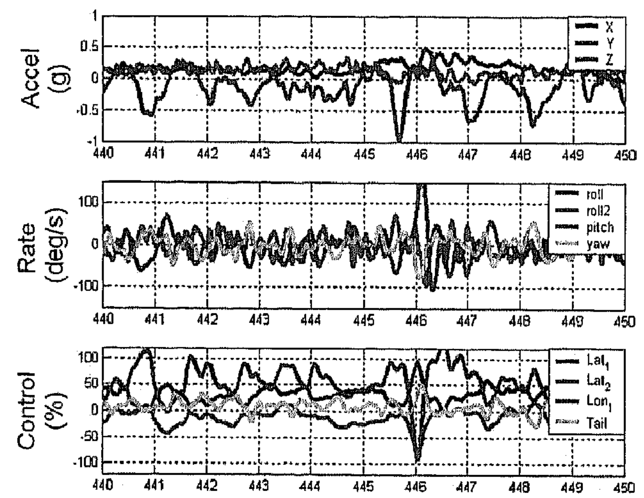

Figure 11. A 10-second time history of flight data from the helicopter flown in a turbulence intensity 14·0% For an IAS of 7·5m/s^{-1}.

correlated with pilot input, as in the first negative peak in Z acceleration at time 371·5s and the associated elevator command. Other responses appear as uncommanded disturbances, such as the negative peak in Z acceleration at 374·5s.

Rate responses for roll, pitch, and yaw are shown in the centre plot, which can be compared with the pilot inputs in the lower plot for a qualitative assessment of the relative magnitudes of the disturbances. Roll rate in particular showed numerous excursions that are uncorrelated to aileron inputs. These excursions were presumably disturbances due to effective rolling moments generated from the spanwise variation of the airflow pitch angle resulting from turbulence. Previous work indicated that MAVs were most sensitive in roll to atmospheric disturbances, compared to pitch and yaw axes, Watkins[13]. Such disturbances caused roll attitude changes that affected the lift vector and accelerate the aircraft away from the desired position in the wind tunnel, as in turning flight. The necessary pilot compensation for such a disturbance included aileron to generate opposing roll moments, but also rudder to generate yaw moments and sideforces needed to compensate for the lateral position deviation. Such required coupling explains the correlation between aileron and rudder in some of the manoeuvre sequences.

The turbulence sensitivity of rotary-wing MAVs appeared to be less than fixed-wing MAVs of similar dimension. Figure 10 shows a 10-second time history of flight data from a helicopter flown at 6·6% turbulence intensity for an IAS of 7·5ms^{-1}. (Note the scaling differences in the vertical axes between the previous data for the fixed wing craft.) Under identical flight conditions the typical translational accelerations of the helicopter are well under half those of the fixed wing and the rotational rates are below one third.

Attempts to fly the fixed wing craft with the tunnel in Configuration B (14% turbulence intensity) were not successful with insufficient data lengths for valid analysis. However this was not the case with the helicopter and Fig. 11 shows a 10-second time history of flight data from a helicopter flown at 14% turbulence intensity in a mean windspeed of 7·5ms^{-1}. The vehicle was flown in this configuration with moderate pilot workload, in contrast to the extreme difficulty in flying the fixed-wing aircraft in similar replicated turbulence.

Most rotary-wing responses to turbulence were benign and readily opposed by pilot action. An exception is seen at time 445·5 seconds in the upper plot, where a disturbance caused a large downward acceleration and negative pitch rate. The pilot response at time 446 seconds was a large nose-up longitudinal cyclic input to arrest the pitching motion combined with collective action to regain lost altitude. Corrective pilot inputs continued for the following second as the helicopter was returned to the desired position and attitude in the tunnel.

9.0 FLAPPING WING TESTS AND INITIAL RESULTS

Two further studies investigating the sensitivity of flapping wing flight to turbulence were conducted. One involved controlled flight experiments in the style of those described previously; the other made use of a dynamic force balance to measure potential body (fuselage) movements. The flying parts of the experiments are on-going (an issue here is the inability to carry the DAQ and instead the video-tracking system will be used to document the motion of the craft).

The flapping mechanism used was the modified working components of a 'Dragonfly'; a commercially available remote-control model. A simple crank mechanism is used to flap the wings, power to which is delivered by an electric motor through a series of reducing gears to achieve the flapping frequency of approximately 6Hz. The standard four wing configuration was removed and replaced by a pair of rigid wings (surface area – 0·01m^2) constructed from balsawood and reinforced with carbon fibre rods. The wings flap through a stroke angle of 50° with the mean positional angle of the wings at 35° dihedral.

The flapping wing craft was attached to a dynamic force balance measuring the lift, drag, pitch and roll responses. Figure 12 shows the craft on the force balance. The balance was designed to be sufficiently stiff and responsive to obtain reliable dynamic data without correction for low mass MAV models or wings. For the model and mount system shown here (total mass 25g) the resonant frequencies of the balance were around 70Hz and were not corrected for, since this is over an order of magnitude greater than the frequencies of interest. Measurements were taken with the craft positioned at several different pitch and roll angles.

Figure 13 shows the lift coefficient, at nominally zero angle of attack, divided by the mean lift coefficient for the whole time sample (60 seconds), and calculated using the conventional aerospace method, where the area is the planform wing area. The graph shows results taken in a mean flow velocity of $4{\cdot}2ms^{-1}$ and a turbulence intensity of 6·6%.

For comparison Fig. 14 shows the lift for the craft with the wings stationary and held rigidly at approximately 10° dihedral, all other variables remaining the same. It should be noted that this is only a preliminary study and results include the inertial forces arising from the flapping mechanism. Other dynamic effects (such as virtual mass estimations) have not been calculated. Further experiments are planned including taking measurements in a vacuum chamber to measure the inertial terms.

10.0 CONCLUDING REMARKS

We have provided a flight test environment which enables MAVs of up to about 1m span to be evaluated either via instrumented flight tests or via direct force and moment measurement on dynamically sensitive balances. From initial flight tests on MAVs we show that when similar-sized rotary-wing and fixed-wing aircraft were flown in identical levels of replicated turbulence, the former showed substantially lower response to disturbances. However, the difficulty in comparing the two responses is exacerbated by a lack of obvious characteristic dimension for each vehicle. Rotor span and wingspan are possible characteristics, as are disc loading and wing loading. Such a comparison does not account for the dissimilarity between the actual airspeed of the fixed wing and that of the spinning rotors, whose speed is much larger and will yield effectively lower turbulence intensities relative to the moving blades. There are also other significant differences between the fixed and rotary craft which include mass, MOI's and dynamics of the rotor head. It is suggested that the comparisons could be made on the basis of payload capability and endurance with perhaps an allowance for physical size. Comparisons made here are thus merely made as subjective observations. This is part of our on-going research where more objective methods of documentation are being assessed Abdulrahim *et al*[14]. Future work includes simulation and experimental testing of methods of mitigating the flight path deviations via sensory inputs (such as inertial, wing bending moments or surface pressures) with suitable compensation via control algorithms.

ACKNOWLEDGMENTS

The authors would like to thank the Asian Office of Aerospace Research & Development, United States Air Force, for providing financial assistance, Satya Mavuri, Ben Loxton, Sridhar Ravi, Alex Fisher and Edward Cruz for logistical support and the administrative and IT staff at RMIT University for their support during the project. The dynamic force balance was designed and commissioned by Robert Richard and was calibrated by Justin Wooley.

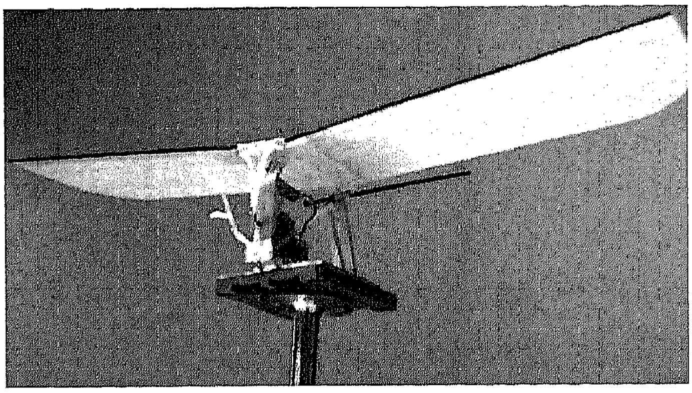

Figure 12. The flapping wing model on the dynamic force balance.

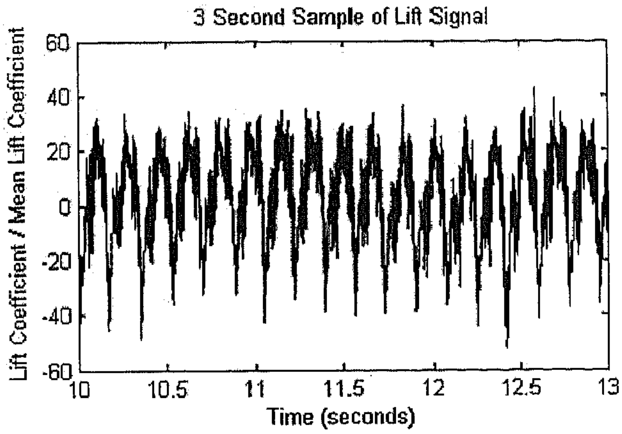

Figure 13. Non-dimensional lift coefficient for the flapping model at ~ 6Hz.

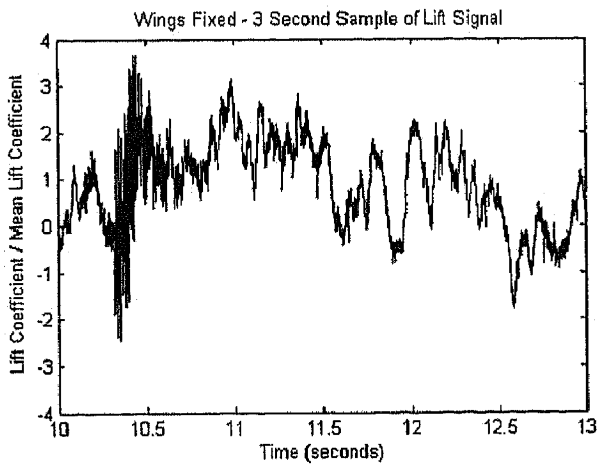

Figure 14. Non-dimensional lift coefficient for the model with wings fixed at a 5° dihedral angle.

REFERENCES

1. BURGER, K. Micro air vehicle demo approaching, *Janes Defence Weekly*, Janes Publications, 12 September 2001, **36**, (14), p 6.
2. HOLMES, J.D. *Wind Loading of Structures*, Spon Press, London, 2001.
3. SUTTON, O.G. *Micrometeorology*, McGraw-Hill Books, New York, USA, 1953.
4. VAN DER HOVEN, I. Power spectrum of horizontal wind speed in the frequency range from 0·0007 to 900 cycles per hour, *J Meteorology*, 1957, 14, pp 160-164.
5. LAWSON, T.V. *Wind Effects on Buildings*, in 2 volumes, Applied Science Publishers, London, UK, 1980.

6. WATKINS, S., MILBANK, J., LOXTON, B.J. and MELBOURNE, W.H. Atmospheric winds and their effects on Micro Air Vehicles, *AIAA J*, November 2006, **11**, (44), pp 2591-2600.
7. MILBANK, J., LOXTON, B.J., WATKINS, S. and MELBOURNE, W.H. Replication of atmospheric conditions for the purpose of testing MAVs, Final Report, USAF Project No: AOARD 05-4075, RMIT University, 2005. Available gratis via http://mams.rmit.edu.au/cibbi0b6g34o.pdf and http://mams.rmit.edu.au/nqjhdfdjn29o.pdf
8. ETKIN, B, Turbulent wind and Its effect on flight, *AIAA J Aircr*, May 1981, **18**, (5), pp 327-345.
9. WATKINS S., LOXTON B., MILBANK, J., MELBOURNE, W.H. and ABDULRAHIM, M. Modelling the atmospheric boundary layer in a large wind tunnel for MAV development 46th AIAA Aerospace Sciences Meeting and Exhibit, 7-10 January 2008, Reno, NV, USA.
10. WATKINS, S., SAUNDERS, J.W., HOFFMANN, P.H. and HOLMES, J.D. Measurements of turbulence experienced by moving vehicles, Part 1. introduction and turbulence intensity, *J Wind Engineering and Industrial Aerodynamics*, 1995, **57**, (1), pp 1– 17.
11. WATKINS S., LOXTON B., MILLBANK J., MELBOURNE W.H. and M. ABDULRAHIM, The turbulent flight environment of MAVs – Flight environment measurements and tunnel replication, 2nd European Conference for Aerospace Sciences (EUCASS, Brussels, Belgium, 1-6 July, 2007.
12. SHORTIS, M.R. and SNOW, W.L. Videometric tracking of wind tunnel aerospace models at NASA Langley Research Centre. The Photogrammetric Record, 1997, **15**, (85), pp 673-689.
13. WATKINS S. Development of a Micro Air Vehicle, *Aeronaut J*, February 2003, **107**, (1068).
14. ABDULRAHIM M., WATKINS S., SEGAL R. and SHERIDAN J. Dynamic sensitivity to atmospheric turbulence of a fixed-wing UAV with varying configuration, presented at the AIAA guidance, Navigation, and Control Conference, 10-13 August, Chicago, Il, USA, 2009 and submitted to the *AIAA J Aircr*.